J S Afr Vet Assoc. 2023;94:78-82
https://doi.org/10.36303/JSAVA.537

J S Afr Vet Assoc
ISSN 2224-9435 EISSN 1019-9128

CASE REPORT

Hepatic myxosarcoma in a domestic shorthair cat

H Moosavian,[1] R Ghiassi,[2] SS Izadi,[3] P Almasi,[1] R Vahabi,[4] M Fazli[5]

[1] *Department of Clinical Pathology, Faculty of Veterinary Medicine, University of Tehran, Iran*
[2] *Department of clinical sciences, faculty of veterinary medicine, Garmsar Branch, Islamic Azad University, Iran*
[3] *Department of Surgery and Radiology, Faculty of Veterinary Medicine, University of Tehran, Iran*
[4] *Department of Pathology and Laboratory Medicine, Isfahan University of Medical Sciences, Iran*
[5] *Department of Biology, Faculty of Basic Science, Islamic Azad University, Iran*
Corresponding author, email: *hrmoosavian@ut.ac.ir*

Myxosarcomas are rare malignant neoplasms of soft connective tissues, and there are no reports of hepatic myxosarcomas in cats. An eight-year-old male, neutered, domestic shorthair cat presented with progressive hyporexia, lethargy, and weight loss. An ultrasonography study showed a large abdominal mass connected to the liver. The cat underwent a laparotomy and the mass was removed. Histopathological evaluation of the mass supported the diagnosis of a myxosarcoma. Tumour cells were positive with vimentin and alcian blue stain, and negative with PAS, pan-cytokeratin, s100, epithelial membrane antigen, and α-smooth muscle actin. The Ki-67 index by immunohistochemistry was 6%. The cat was euthanased due to severe lethargy and recumbency. Myxoid soft tissue neoplasms are very rare in cats, and to the best of our knowledge, this is the first report of a hepatic myxosarcoma in a cat. In the present case, the diagnosis was made based on histopathological and immunohistochemical findings and an alcian blue-positive supporting matrix.

Keywords: cats, feline, Ki-67 , liver, myxosarcoma, immunohistochemistry

Introduction

Myxosarcomas are soft tissue sarcomas which are rare in dogs and cats. The neoplastic cells originate from fibroblasts and produce an abundant myxoid matrix composed of mucopolysaccharides (Goldschmidt & Hendrick 2002). The majority of myxosarcoma cases in animals have been documented in dogs, and the most often reported anatomical locations are the trunk and limbs. Myxosarcomas in dogs were reported in other organs, including the brain, spleen, spine, vertebra, heart, eye, lung, and temporomandibular joint (Iwaki et al. 2019). However, based on the literature reviewed, there are few reports of myxosarcomas in the cat. Myxosarcomas in cats have been reported in the kidney, muscle and retroperitoneum (Hixson et al. 2022; Madere et al. 2020; Manfredi et al. 2015). Furthermore, myxosarcoma is reported as one of the feline injection-site sarcoma histological types (Saba 2017). To the best of our knowledge, there are no reports of hepatic myxosarcomas in cats and there is also no comprehensive survey of myxosarcoma characterisation in cats. The current report describes the clinical and laboratory findings of the first documented case of a primary hepatic myxosarcoma in a cat.

Case presentation

An eight-year-old male, neutered, domestic shorthair cat presented with a three-month history of progressive hyporexia, lethargy, weight loss, and intermittent vomiting. The cat's vaccination status was adequate, and there was no history of notable medical illnesses. On physical examination, the cat was in poor body condition (body weight of 3 100 g; body condition score of 3 out of 9). No abnormalities were noted other than hyporexia, lethargy, a loss of more than 2 kg in body weight in the preceding months, mild dehydration (< 5%), and a mild amount of dental tartar. There were no palpable lymph nodes, and a normal cardiac rhythm was detected during the auscultation of the thorax.

Management and outcome

The complete blood count (CBC) results were unremarkable and the biochemistry panel revealed an elevated alkaline phosphatase, gamma-glutamyltransferase, and lactate dehydrogenase (ALP: 90 U/L, reference interval [RI]: 0 to 62 U/L, GGT: 8.6 U/L, RI: 0 to 6 U/L and LDH: 371 U/L, RI: 46 to 350 U/L) (Krimer 2011), indicating possible hepatobiliary damage. Abdominal ultrasonography revealed a well-defined abdominal mass (maximum diameter 15 cm), arising from the right liver lobe. Based on the abdominal ultrasound and thoracic radiographs, the patient had no evidence of metastatic disease or involvement of organs other than the liver.

The cat's dehydration was managed with intravenous fluid therapy (0.9% NaCl at rates of up to 1.5 ml/kg/hr, and duphalyte solution at rates of up to 0.5 ml/kg/hr). Exploratory laparotomy revealed an enlarged abdominal gelatinous mass arising from the liver. The mass was removed surgically with a 5 mm resection margin and submitted for histopathology. In general, gross pathology revealed the excised mass to be a smooth, gelatinous, light yellow mass, measuring 15.511.5×8 cm and weighing 600 grams. (Figures 1A and 1B). On sectioned surfaces, exudation of clear viscous fluid was seen. Macroscopic examination revealed three distinct parts in the mass (Figure 1C): (Part 1): a large yellow gelatinous part; (Part 2): a reddish-brown part with remnants of liver tissue; and (Part 3): a white multilobular part, with a relatively firm consistency.

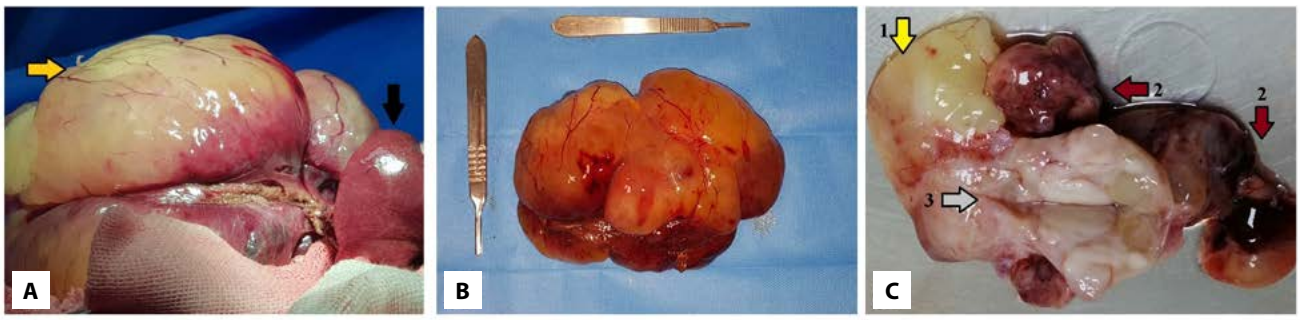

Figure 1: Macroscopic findings of the abdominal mass
(A) A large abdominal mass (orange arrow), attached to the liver (black arrow) was found in the exploratory laparotomy; (B) The large abdominal mass was observed to be a smooth, gelatinous mass, and pale yellow in colour, measuring 15.5×11.5×8 cm; (C) Macroscopic examination revealed three different parts in the mass: (1): A large yellow gelatinous part (yellow arrow), (2): A brown hyperaemic part with residuals of liver tissue (brown arrow), and (3): A white parenchymatous part, with a relatively firm consistency (white arrow)

Impression smears from the mass were submitted for cytological study. Slides were stained with a commercially available modified Giemsa stain (Sigma).

The impression smears showed irregularly shaped spindle cells found both individually and within small clusters (Figure 2A). Typically, the cytoplasm had wispy edges and cells had cytoplasmic vacuoles. The nuclei were medium-sized and centrally located. A prominent nucleolus was seen in some cells. In some areas, the neoplastic cells were associated with and surrounded by abundant acellular pale eosinophilic matrix. The cytology findings were compatible with a soft tissue mesenchymal neoplasm.

The microscopical examination was performed on the formalin-fixed and paraffin wax-embedded tissue. 5-µm thick sections were slide-mounted and stained with hematoxylin and eosin (H & E). The different components of the mass were examined separately. Part 1 (Figure 1C, Part 1) exhibited abundant acellular to poorly cellular pale eosinophilic stroma with focal bile duct proliferation (Figures 2B and 2C). In part 2 (Figure 1C, Part 2) there was a myxoid stroma with a moderately dense proliferation of spindle cells in an erythrocyte-rich background. The cells were loosely arranged and included wispy eosinophilic cytoplasm and oval dense basophilic nuclei with prominent nucleoli. There was evidence of moderate to severe pleomorphism. Discrete hepatic cords were observed among the neoplastic cells (Figure 2D). Part 3 (Figure

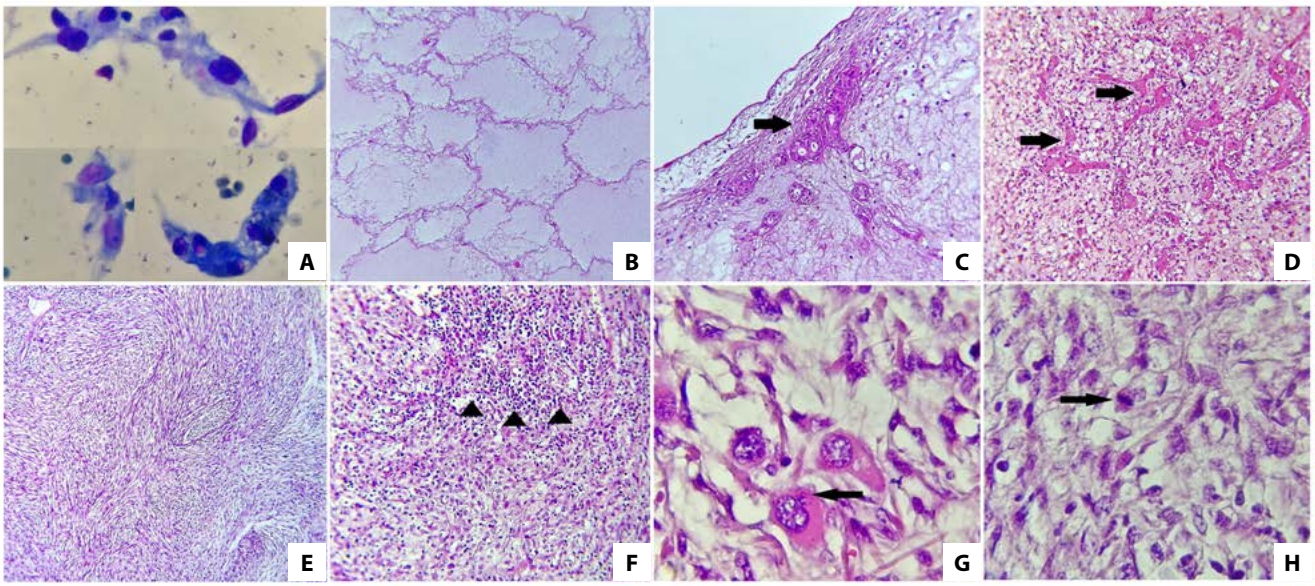

Figure 2: Photomicrographs of and tissue imprint, Giemsa staining (A), and haematoxylin and eosin-stained hepatic mass (B–H). Photomicrographs B and C are histopathology sections taken from the gelatinous part (Figure 1C, 1), Photomicrograph D, taken from the brown hyperaemic part (Figure 1C, 2), and Photomicrograph E–H, taken from the white solid part (Figure 1C, 3) of the abdominal mass
(A) Impression smear and cytology study (Giemsa stain), from the abdominal mass. Some irregularly shaped spindle cells were found in small aggregates, the cells had moderate nuclei with blue cytoplasm, cytoplasmic vacuoles, and wispy cytoplasmic borders extending from the nucleus. Prominent nucleolus was seen in some cells. (×1000 magnification); (B) Acellular to a poorly cellular area with a marked abundance of the extracellular myxoid matrix (asterisk) (×200 magnification); (C) Myxoid matrix (asterisk), with focal bile duct proliferation (arrow) (×200 magnification); (D) The proliferation of stellate to spindle-shaped fibroblasts loosely arranged in an abundant myxoid matrix, and invasion of neoplastic cells with remnant hepatic parenchyma (arrow) (×200 magnification); (E) More cellular areas (related to the Part C, Figure 1), composed of pleomorphic spindle cells in a myxoid stroma (×100 magnification); (F) Mononuclear cell infiltration (arrow) in the cellular area (×200 magnification); (G) Variation in the size and shape of neoplastic cells, moderate to marked nuclear pleomorphism, and the presence of micronuclei in a few neoplastic cells (arrow) (×1000 magnification); (H) Rare mitotic figures (arrow) (×1000 magnification)

Table I: Primary antibodies used for immunohistochemical evaluation of feline hepatic myxosarcoma

Antibody*		Dilution	Source	Positive control**	Negative control	Results
Vimentin	Mouse Mab, IgG1	Ready-to-use	*Zytomed* Systems	In. C, smooth muscle cells from arteries	In. C, hepatocytes	Positive
Ki-67	Mouse Mab, IgG1-κ	1:150	Zeta	Ex. C, *cat's tonsil*	In. C, hepatocytes	Positive
Pan-cytokeratin (AE1 and AE3)	Mouse Mab, IgG1	Ready-to-use	*Zytomed* Systems	In. C, hepatocytes	In. C, smooth muscle cells from arteries	Negative
S100	Mouse Mab, IgG2a	Ready-to-use	*Zytomed* Systems	*Ex. C. cat's normal adipose tissue*	In. C, hepatocytes	Negative
EMA	Mouse Mab, IgG1-κ	1:50	Diagnostic Biosystems	In. C, hepatocytes	In. C, Smooth muscle cells from arteries	Negative
α-SMA	Mouse Mab, IgG2a-κ	1:50	Diagnostic Biosystems	In. C, smooth muscle cells from arteries	In. C, hepatocytes	Negative

1C, Part 3) was hypercellular, with greater pleomorphism of cells in a myxoid stroma (Figures 2E, 2F, 2G and 2H).

Additional histological findings included the presence of micronuclei in a few large cells, the presence of mitotic figures, averaging 1 per 10 high power fields (2.37 mm^2), and mononuclear cell infiltration (Figures 2F, 2G, and 2H).

The neoplasm was graded and classified based on the cutaneous and subcutaneous soft tissue sarcoma (STS) grading system in cats (Dobromylskyj et al. 2020), based on the inflammation score, presence and extent of necrosis within the neoplasm, and mitotic rate. Based on the mild inflammation (Inflammation Score: 2/3), low number of mitotic figures in the hyper-cellular areas shown in Figure 2H (1 mitosis per 10 HPF [FN22/40_ objective], Mitotic Score 1/3) and mild necrosis (Tumour Necrosis Score: 1/2), the total score was 4/8, and the sarcoma was designated as grade 2/3 (intermediate) overall. Neoplastic tissue was present in the excisional margins, and chemotherapy was recommended. However, the owner refused further treatment.

To further characterise the neoplasm, alcian blue, Periodic acid–Schiff (PAS), and immunohistochemical (IHC) staining were

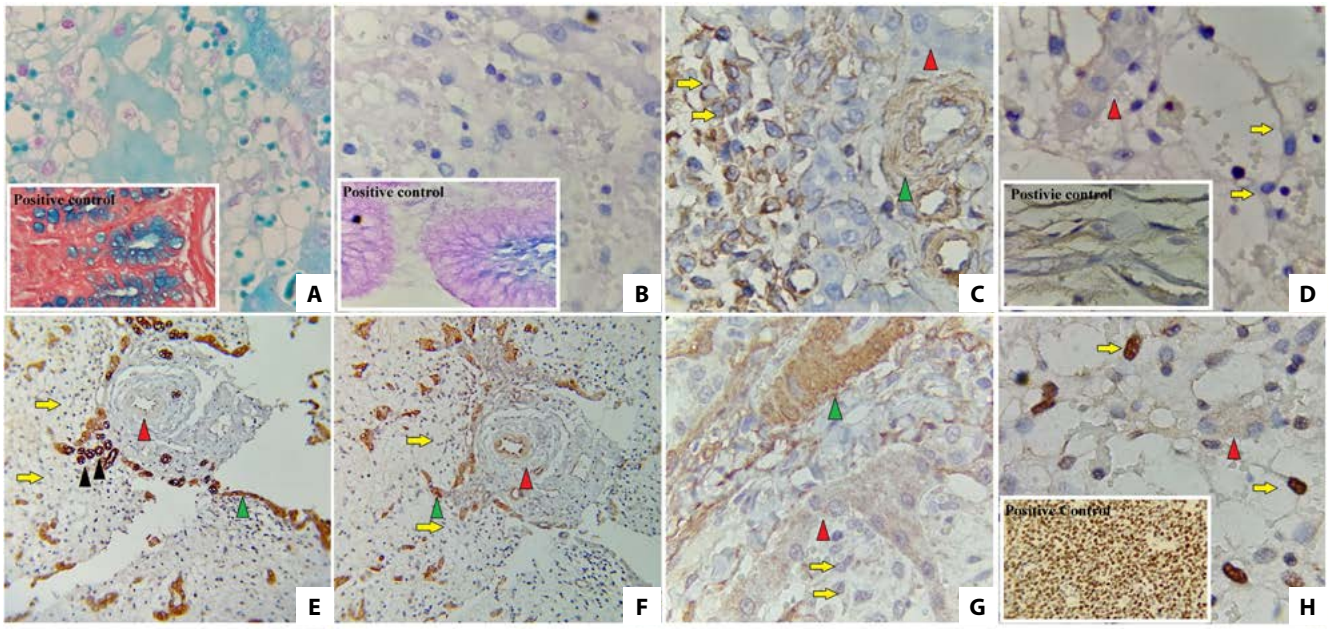

Figure 3: Photomicrographs of alcian blue and PAS staining, and immunohistochemical expression of vimentin, S100, Pan-cytokeratin, EMA, SMA, and Ki-67 in feline myxosarcoma
(A) Strong reactivity to alcian blue histochemical staining of the myxomatous matrix, confirming the presence of mucin (×1000 magnification); colonic mucosa was used as the external positive control; (B) No reactivity to PAS staining (×1000 magnification); gastric mucosa was used as the external positive control; (C) Positive immunolabelling with vimentin (yellow arrow), (×1000 magnification); smooth muscle cells from arteries were used as the internal positive control (green arrow), and hepatocytes were used as internal negative control (red arrow); (D) Negative immunolabelling with S100 (yellow arrow), (×1000 magnification); cat's normal adipose tissue was used as the external positive control, and hepatocytes were used as the internal negative control (red arrow); (E) Negative immunoreactivity of neoplastic cells (yellow arrow), and positive immunolabelling of proliferating bile ducts (bile duct hyperplasia) for Pan-cytokeratin (black arrowhead). (×200 magnification); Hepatocytes were used as the internal positive control (green arrow), and smooth muscle cells from arteries were used as internal negative control (red arrow); (F) Negative immunoreactivity with EMA (yellow arrow), (×200 magnification); hepatocytes were used as the internal positive control (green arrow), and smooth muscle cells from arteries were used as the internal negative control (red arrow); (G) Negative immunoreactivity with SMA (yellow arrow), (×1000 magnification); smooth muscle cells from arteries were used as the internal positive control (green arrow), and hepatocytes were used as the internal negative control (red arrow); (H) Positive immunostaining for Ki-67, as diffusely granular nuclear staining in some tumour cells (yellow arrow), (×1000 magnification); Cat's tonsil was used as the external positive control, and hepatocytes were used as the internal negative control (red arrow).

performed on paraffin-embedded tissue. Positive staining as a light blue hue with alcian blue staining proved the existence of a myxoid matrix and the tissue sections were negative with PAS staining. Gastric and colonic mucosa were used as the positive controls for PAS and alcian blue staining, respectively (Figures 3A and 3B). In the IHC study (Table I), the neoplastic cells showed strong immunoreactivity to vimentin and no immunoreactivity to s100, pan-cytokeratin, epithelial membrane antigen (EMA), and α-smooth muscle actin (αSMA) (Figure 3). Pan-cytokeratin antibody positively immune-labelled bile ducts and bile duct proliferation was confirmed (Figure 3E). The Ki-67 index (percentage of positive cells in 1 000 neoplastic cells, assessed using IHC and light microscopy, high power field) was 6% (Figure 3H). Based on morphological and staining characteristics, the final diagnosis of myxosarcoma was made.

Progressive hyporexia and weight loss were seen in the patient one month after surgery and the owner decided on euthanasia. The autopsy examination revealed no lesions in the other abdominal organs. Multifocal areas of necrosis and petechial haemorrhage were seen in the liver. Histopathological evaluation of the previous surgical margins confirmed the presence of neoplastic cells in the liver parenchyma.

Discussion

Hepatic neoplasms in dogs and cats include primary and metastatic tumours. The prevalence of metastatic neoplasms is higher than primary neoplasms in the liver in dogs and cats. Primary hepatic neoplasms include hepatocellular, bile duct, mesenchymal, and neuroendocrine tumours accounting for 0.6% to 1.5% and 1.0% to 2.9% of all canine and feline tumours, respectively. While the majority of primary hepatic neoplasms in dogs are malignant, in cats they are usually benign, with biliary cystadenoma being more common in cats (Cullen & Popp 2002; Hammer & Sikkema 1995). Not only are primary liver sarcoma rare in cats, but also, myxosarcomas are extremely rare in cats. To date, no previous reports have described a primary hepatic myxosarcoma in a cat. In the present study, the clinical, haematology, and biochemistry findings were all non-specific. Histologically, the neoplasm had a diffuse myxoid matrix that stained alcian blue positive and no reaction to PAS, which is the usual histological feature of myxoma. In general, mucins produced by the mesenchymal cells are positive with alcian blue staining, but negative to weakly positive with PAS staining. However, epithelial-derived mucins are positive for both alcian blue and PAS stains (Astudillo et al. 2015).

In a few neoplastic cells, micronuclei were seen. Tumour cells are prone to chromosomal instability and micronuclei formation is a feature of malignancy (Tang et al. 2018). Ductular proliferation has been reported in long-standing biliary diseases such as chronic cholangitis, primary biliary cirrhosis, primary sclerosing cholangitis, and extrahepatic biliary obstruction (Chen et al. 2006, Cullen 2009). In the present study, the neoplastic invasion to the liver may have caused biliary obstruction and cholestasis, and so had an indirect role in the ductular reaction.

There were no definitive areas of cellular or vascular patterns diagnostic of haemangiosarcoma, fibrosarcoma, liposarcoma, leiomyosarcoma or rhabdomyosarcoma.

IHC revealed the neoplastic cells to express vimentin but not pan-cytokeratin, confirming a mesenchymal origin. Neoplastic cells were not immunoreactive for s100, EMA, and αSMA, reducing the likelihood of neuronal, perineural, adipocyte, melanocyte, chondrocyte, myopericytoma, leiomyosarcoma, or myoepithelial origin. Campos et al. (2015) reported that neoplastic cells in a myxosarcoma showed vimentin-positive immunoreactivity, and did not label with αSMA. Hepatic myxosarcoma was diagnosed based on gross, histological, special stain and immunohistochemical findings. Because myxosarcoma is relatively uncommon in animals, particularly cats, there is a dearth of knowledge about its clinical manifestations, prognosis, and other histological abnormalities in cats. Out of three cases of myxosarcoma reported in cats, two cats recovered from surgery without complication. Patients were monitored for six months in one study and 14 months in another study, and no signs of disease and metastasis were detected in patients (Madere et al. 2020; Manfredi et al. 2015).

In another study, aggressive recurrence of retroperitoneal myxosarcoma in a cat that was previously excised was reported (Hixson et al. 2022).

In a report of ten dogs with skin myxosarcomas, the median survival time was 66 weeks (Bostock & Dye 1980).

In the histopathology evaluation of visceral sarcomas in cats and dogs, there is currently no a comprehensive scoring system. In a recent study in dogs, visceral sarcomas were graded using the previously described scheme for soft tissue sarcomas of the skin and subcutis. The results showed the grading system can be prognostic for the visceral sarcoma (Linden et al. 2019).

In the present case, the neoplasm was graded and classified based on the cutaneous and subcutaneous STS grading system in cats (Dobromylskyj et al. 2020).

The myxosarcoma was classified as grade II based on the evaluation of the inflammation, necrosis, and mitotic indices. However, large tumour size, local invasion of neoplastic cells to the liver, and marked cellular pleomorphism were poor prognostic factors. It seems that probably other factors such as delay in cancer diagnosis and the presence of neoplastic cells in surgical margin were negative prognostic factors.

In the present study, despite the large size of the mass, the number of Ki-67-positive cells was low (6%) and no evidence of metastasis was seen. Based on the scientific literature in veterinary medicine, the cut-offs in defining a low or high Ki-67 proliferation index is not well-established or universally agreed upon. High Ki-67 proliferation index in feline injection site fibrosarcomas have been shown to correlate with a higher malignancy grade, inflammation score, necrosis score and poorer prognosis.

The mean Ki-67 index in feline injection site fibrosarcomas has been reported as 6.64 ± 3.31, 15.25 ± 5.36 and 38.4 ± 14.4 in tumours grade I, II and III, respectively (Mikiewicz et al. 2023).

Conclusion

Myxoid soft tissue neoplasms are very rare in cats, and to the best of our knowledge, this is the first report of a hepatic myxosarcoma in a cat. In the present case, histopathological, histochemical, and immunohistochemical techniques enabled the diagnosis of a rare feline hepatic myxosarcoma. The production of extracellular myxoid matrix by a myxoid mesenchymal neoplasm can be highlighted by alcian blue-positive staining and weak or no reaction to PAS. The results of the present study can improve our knowledge about morphological and histopathological characteristics of myxosarcoma in cats. However, further investigation in feline visceral soft tissue sarcoma will be required to determine whether grading system, Ki-67, and surgical margins may improve determination of prognosis.

Conflict of interest

The authors have declared that no competing interest exists.

Funding source

This case report received no specific grant from any funding agency in the public, commercial, or not-for-profit sectors.

Ethical approval

Owners' consent was obtained for the procedures undertaken and the use of the data for research purposes. Established internationally recognised high standards of veterinary clinical patient care were followed. Ethical approval from a committee was therefore not specifically required.

References

Astudillo, V.G., Schaffer-White, A., Allavena, R., et al., 2015, Multiple intra-abdominal serosal myxosarcomas in two koalas (*Phascolarctos cinereus*), *J Comp Pathol* 152(2-3), 283–286. https://doi.org/10.1016/j.jcpa.2015.01.004.

Bostock, D.E., Dye, M.T., 1980, Prognosis after surgical excision of canine fibrous connective tissue sarcomas, *Vet Pathol* 17(5), 581–588. https://doi.org/10.1177/030098588001700507.

Campos, C.B., Nunes, F.C., Gamba, C.O., et al., 2015, Canine low-grade intra-orbital myxosarcoma: case report, *Vet Ophthalmol* 18(3), 251–253. https://doi.org/10.1111/vop.12183.

Chen, Y.K., Zhao, X.X., Li, J.G., et al., 2006, Ductular proliferation in liver tissues with severe chronic hepatitis B: an immunohistochemical study, *World J Gastroenterol* 12(9), 1443–1446. https://doi.org/10.3748/wjg.v12.i9.1443.

Cullen, J.M., 2009, Summary of the World Small Animal Veterinary Association standardization committee guide to classification of liver disease in dogs and cats, *Vet Clin North Am Small Anim Pract* 39(3), 395–418. https://doi.org/10.1016/j.cvsm.2009.02.003.

Cullen, J.M., Popp, J.A., 2002, Tumors of the liver and gall bladder, in D.J. Meuten, *Tumors in domestic animals*, pp. 483–508. https://doi.org/10.1002/9780470376928.ch9.

Dobromylskyj, M.J., Richards, V., Smith, K.C., 2020, Prognostic factors and proposed grading system for cutaneous and subcutaneous soft tissue sarcomas in cats, based on a retrospective study, *J Feline Med Surg* 23(2), 168–174. https://doi.org/10.1177/1098612X20942393.

Goldschmidt, M.H., Hendrick, M.J., 2002, 'Tumors of the skin and soft tissues', in D.J. Meuten, *Tumors in domestic animals*, pp. 45–117. https://doi.org/10.1002/9780470376928.ch2.

Hammer, A.S., Sikkema, D.A., 1995, Hepatic neoplasia in the dog and cat, *Vet Clin North Am Small Anim Pract* 25(2), 419–435. https://doi.org/10.1016/S0195-5616(95)50035-X.

Hixson, H., Coutermarsh-Ott, S., Ciepluch, B., et al., 2022, Retroperitoneal myxosarcoma in a cat, *Clin Case Rep* 10(7), e6063. https://doi.org/10.1002/ccr3.6063.

Iwaki, Y., Lindley, S., Smith, A., et al., 2019, Canine myxosarcomas, a retrospective analysis of 32 dogs (2003-2018), *BMC Vet Res* 15(1), 217. https://doi.org/10.1186/s12917-019-1956-z.

Krimer, P.M., 2011, Generating and interpreting test results: test validity, quality control, reference values, and basic epidemiology, in K.S. Latimer, *Duncan and Prasse's veterinary laboratory medicine: clinical pathology*, pp. 365–382.

Linden, D., Liptak, J.M., Vinayak, A., et al., 2019, Outcomes and prognostic variables associated with primary abdominal visceral soft tissue sarcomas in dogs: A Veterinary Society of Surgical Oncology retrospective study, *Vet Comp Oncol* 17(3), 265–270. https://doi.org/10.1111/vco.12456.

Madere, B.C., Dedeaux, A., Negrao Watanabe, T.T., et al., 2020, Myxosarcoma associated with the kidney in a cat: case report, *J Am Anim Hosp Assoc* 56(2), e56202. https://doi.org/10.5326/JAAHA-MS-6863.

Manfredi, S., Volta, A., Fabbi, M., et al., 2015, What is your diagnosis? Myxosarcoma in a cat, *J Am Vet Med Assoc* 247(6), 597–599. https://doi.org/10.2460/javma.247.6.597.

Mikiewicz, M., Paździor-Czapula, K., Fiedorowicz, J., et al., 2023, Metallothionein expression in feline injection site fibrosarcomas, *BMC Vet Res* 19(1), 42. https://doi.org/10.1186/s12917-023-03604-5.

Saba, C.F., 2017, Vaccine-associated feline sarcoma: current perspectives, *Vet Med (Auckl)* 8(13), 13–20. https://doi.org/10.2147/VMRR.S116556.

Tang, Z., Yang, J., Wang, X., et al., 2018, Active DNA end processing in micronuclei of ovarian cancer cells, *BMC Cancer* 18(1), 426. https://doi.org/10.1186/s12885-018-4347-0.